Technology and Health Care 28 (2020) S245–S251
DOI 10.3233/THC-209025
IOS Press

The effect of external voltage stimulation on absence seizures

Bing Hu[a,*], Dingjiang Wang[a,*] and Qianqian Shi[b]
[a]*Department of Applied Mathematics, Zhejiang University of Technology, Hangzhou, Zhejiang, 310023, China*
[b]*College of Informatics, Huazhong Agricultural University, Wuhan, 430070, China*

Abstract.
BACKGROUND: Absence epilepsy (AE) is a systemic disease of the brain, which mainly occurs during childhood and adolescence. The control mechanism is still unclear, and few theoretical studies have been conducted to investigate this.
OBJECTIVE: In this paper, we employed external direct voltage stimulation in the subthalamic nucleus to explore mechanisms that inhibit absence seizures.
METHODS: All simulation results are obtained by the four-order Runge-Kutta method in the MATLAB environment. The inhibition mechanism can be inferred from the results.
RESULTS: We found that the seizures may be inhibited by tuning the strength of the voltage to suitable ranges. This regulation may be achieved through the competition between the inhibitory projections from the basal ganglia to the thalamus.
CONCLUSION: Because the mechanism underlying the treatment of epilepsy with a uniform direct current electric field is unclear, we hope that these results can inspire further experimental studies.

Keywords: Absence seizure, subthalamic nucleus, voltage, control, network

1. Introduction

Absence epilepsy (AE) is a systemic disease of the brain, which mainly occurs during childhood and adolescence [1] and without any previous symptoms. AE patients often exhibit loss of consciousness, activity interruption, motionlessness, a slight loss of tension, and tonic-clonic seizures for short durations. Its main clinical electrophysiological features are bilateral synchronous slow spike-wave discharges (SWDs), the frequency of which is very low, approximately 2–4 Hz [2]. Many experiments have implied that AE may be induced via abnormal discharge activity in the thalamocortical circuits (TC) of the bilateral parts of the brain. Many large-scale thalamocortical computational models have been employed to explore the onset mechanism of epilepsy, and the results obtained can be compared well to experimental experiments and observations [3–5]. Marten et al. showed that AE can result from abnormal excitatory inputs from the cortex to the thalamic relay nucleus (SRN) [6,7]. Chen et al. found that by changing the inhibitory coupling strength and the signal transmission delay from the thalamic reticular nucleus (TRN) to the SRN, the brain may be changed into a seizure state [8]. Hu et al. observed that seizure states in a TC model can be induced by varying the coupling strengths of some excitatory pathways connected to

*Corresponding authors: Bing Hu and Dingjiang Wang, Department of Applied Mathematics, Zhejiang University of Technology, Hangzhou, Zhejiang, 310023, China. E-mails: djhubingst@163.com and wangdingj@126.com.

the SRN [9]. However, the control mechanism of epilepsy is still unclear, and few theoretical studies have been conducted to investigate this mechanism.

Deep brain stimulation (DBS) is a common method to control intractable epilepsy with clear effects on the patient [10]. For example, Vesper et al. treated a patient with progressive myoclonic epilepsy by using chronic high frequency DBS and found that bilateral unipolar DBS can reduce the frequency and strength of seizures by 50% by stimulating the subthalamic nucleus (STN) [11]. In 2013, Jou et al. employed high frequency and low intensity current in the left anterior thalamic nucleus of a rat model and found that seizures can be effectively reduced [12]. Feng et al. used DBS on the dorsal part of the STN in a transgenic rat model to explore its controlling effects on drug-resistant epilepsy [13]. Pasnicu et al. showed that low- and high-frequency stimulation of the central nucleus of the thalamus (THA) can effectively suppress seizure phenomena and their frequencies [14]. This is the first time that DBS was shown to effectively inhibit local seizures by acting on the ipsilateral central nucleus of the thalamus. In theoretical research, Chen et al. showed that the basal ganglia (BAG) may have a bidirectional, mediated function on absence seizures [8] and that the direct pallido-cortical pathway can regulate seizures [15]. Recently, Sorokin et al. found a bidirectional adjustment phenomenon in a generalized epilepsy network via rapid real-time switching of phasic firing and tonic firing modes in the TC [16]. Hu et al. found that AE may be inhibited by adjusting the firing ability of neurons of the thalamus and striatum [17]. Due to technical challenges posed by uniform direct current (DC) electric field invasive cortical stimulation, few studies have investigated DC field control of seizures, especially in the field of mathematical theoretical modelling. Ghai et al. found that DC fields can mediate low-calcium epileptiform activity by directly polarizing CA1 pyramidal neurons [18]. Radman et al. found that cortical neuron morphology and type are key to determining the sensitivity to supra- and sub-threshold uniform electric fields [19]. Liebetanz et al. noted that the anticonvulsant roles of transcranial direct-current stimulation (tDCS) depend on stimulation duration and current strength, which may point to tDCS as a potential tool to control partial seizures [20]. Recently, some studies focused on the optogenetic control (OPC) of epilepsy [21]. Paz et al. found that closed-loop OPC of the thalamus may be an effective scheme for interrupting seizures after cortical injury [22]. However, the therapeutic mechanism of DC stimulation is still unclear and should be further explored.

In this paper, by employed a classical cerebral basal ganglia-thalamocortical (BGTC) network [8,9,15], we will explore the mechanism to control AE by employing external DC stimulation on the STN. We observed that the seizure may be well inhibited by adjusting the voltage strength properly, and the control mechanism may be inferred from the model together with the numerical results. This model and method may provide a unified framework to investigate similar problems in the future.

2. Model and method

2.1. Mathematical theory model

Figure 1 shows the model used in this paper [8,9,15]. It consists of nine nerve nuclei; for the sake of brevity, we denote them as follows: $s =$ SRN; $r =$ TRN; $i =$ inhibitory interneurons (IIN); $e =$ excitatory pyramidal neurons (EPN); $d_1 =$ striatal D1 neurons (SD1); $d_2 =$ striatal D2 neurons (SD2); $\varsigma =$ STN; $p_1 =$ substantia nigra pars reticulata (SNr); $p_2 =$ globus pallidus external (GPe). Lines with arrowheads indicate excitatory inputs regulated by glutamate; lines with dots are inhibitory inputs regulated by γ-aminobutyric acid-A ($GABA_A$) or by γ-aminobutyric acid-B ($GABA_B$) receptors. V is the external stimulation voltage acting on the STN.

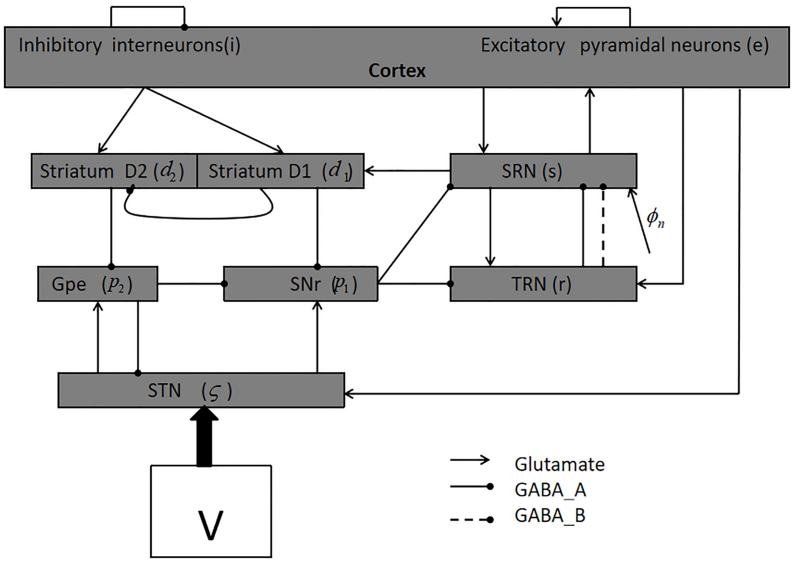

Fig. 1. The basal ganglia-thalamocortical network (BGTC). s = SRN; r = TRN; i = IIN; e = EPN; d_1 = SD1; d_2 = SD2; ς = STN; p_1 = SNr; p_2 = GPe. There are three types of synaptic couplings in this neural model, and we use different connecting lines to distinguish them; lines with arrowheads indicate excitatory inputs regulated by glutamate, and lines with dots are inhibitory inputs regulated by γ-aminobutyric acid-A ($GABA_A$) or γ-aminobutyric acid-B ($GABA_B$) receptors. V is the DC voltage acting on the STN.

We use the following first-order equations in numerical calculations [8,9,15,23]:

$$\frac{d\phi_e(t)}{dt} = \dot{\phi}_e(t)$$

$$\frac{d\dot{\phi}_e(t)}{dt} = \gamma_e^2\left[-\phi_e(t) + F(V_e(t))\right] - 2\gamma_e\dot{\phi}_e(t)$$

$$\frac{dX(t)}{dt} = \dot{X}(t)$$

$$X(t) = \left[V_e(t), V_{d_1}(t), V_{d_2}(t), V_{p_1}(t), V_{p_2}(t), V_\zeta(t), V_r(t), V_s(t)\right]^T$$

$$\frac{d\dot{V}_e(t)}{dt} = \alpha\beta\left(\nu_{ee}\phi_e + \nu_{ei}F(V_e(t)) + \nu_{es}F(V_s(t)) - V_e(t)\right) - (\alpha+\beta)\dot{V}_e(t)$$

$$\frac{d\dot{V}_{d_1}(t)}{dt} = \alpha\beta\left(\nu_{d_1e}\phi_e + \nu_{d_1d_1}F(V_{d_1}(t)) + \nu_{d_1s}F(V_s(t)) - V_{d_1}(t)\right) - (\alpha+\beta)\dot{V}_{d_1}(t)$$

$$\frac{d\dot{V}_{d_2}(t)}{dt} = \alpha\beta\left(\nu_{d_2e}\phi_e + \nu_{d_2d_2}F(V_{d_2}(t)) + \nu_{d_2s}F(V_s(t)) - V_{d_2}(t)\right) - (\alpha+\beta)\dot{V}_{d_2}(t)$$

$$\frac{d\dot{V}_{p_1}(t)}{dt} = \alpha\beta\left(\nu_{p_1d_1}F(V_{d_1}(t)) + \nu_{p_1p_2}F(V_{p_2}(t)) + \nu_{p_1\zeta}F(V_\zeta(t)) - V_{p_1}(t)\right) - (\alpha+\beta)\dot{V}_{p_1}(t)$$

$$\frac{d\dot{V}_{p_2}(t)}{dt} = \alpha\beta\left(\nu_{p_2d_2}F(V_{d_2}(t)) + \nu_{p_2p_2}F(V_{p_2}(t)) + \nu_{p_2\zeta}F(V_\zeta(t)) - V_{p_2}(t)\right) - (\alpha+\beta)\dot{V}_{p_2}(t)$$

$$\frac{d\dot{V}_\zeta(t)}{dt} = \alpha\beta\left(\nu_{\zeta e}\phi_e + \nu_{\zeta p_2}F(V_{p_2}(t)) - V_\zeta(t) + V\right) - (\alpha+\beta)\dot{V}_\zeta(t)$$

$$\frac{d\dot{V}_r(t)}{dt} = \alpha\beta\left(\nu_{re}\phi_e + \nu_{rp_1}F\left(V_{p_1}(t)\right) + \nu_{rs}F\left(V_s(t)\right) - V_r(t)\right) - (\alpha+\beta)\dot{V}_r(t)$$

$$\frac{d\dot{V}_s(t)}{dt} = \alpha\beta\left(\nu_{se}\phi_e + \nu_{sp_1}F\left(V_{p_1}(t)\right) + \nu_{sr}^{A}F\left(V_r\right) + \nu_{sr}^{B}F\left(V_r(T-\tau)\right) - V_s(t) + \phi_n\right) - (\alpha+\beta)\dot{V}_s(t)$$

For each nerve nucleus "a", $V_a(t)$ is the cell body electric potential, F is a sigmoid function defined as a function of $V_a(t)$:

$$F\left(V_a(t)\right) = \frac{Q_a^{\max}}{1+\exp\left[-\left(V_a(t)-\theta_a\right)/\sigma\right]}$$

$Q_a^{\max}$ represents the maximum discharge rate, σ denotes the standard deviation of the discharge threshold, θ_a is the average threshold electric potential, γ_e is the damping ratio of the STN. α and β represent the attenuation and gain rates of $Va(t)$. v_{ab} corresponds to the connection weight from population "b" to population "a". $\phi_e(t)$ is the output pulse rate of the EPN. τ is a delay in the "*TRN* $\rightarrow$ *SRN*". ϕ_n represents non-specific subthalamic nucleus input.

2.2. Numerical calculation method and data

The four-order Runge-Kutta method is employed to solve the above equations with a step size of $\Delta t =$ 0.00005 s, specific ideas of which can refer to [8,9,15]. The data used in this article are listed in the following [8,9,15,23]: $Q_e^{\max}, Q_i^{\max} = 250$ Hz, $Q_{d_1}^{\max}, Q_{d_2}^{\max} = 65$ Hz, $Q_{\varsigma}^{\max} = 500$ Hz, $Q_{p_1}^{\max} = 250$ Hz, $Q_{p_2}^{\max} = 300$ Hz, $Q_r^{\max} = 250$ Hz, $Q_s^{\max} = 250$ Hz, $\theta_{\varsigma} = 10$ mV, $\theta_{d_1}, \theta_{d_2} = 19$ mV, $\theta_s = 15$ mV, $\theta_{p_1} =$ 10 mV, $\theta_r = 15$ mV, $\theta_{p_2} = 9$ mV, $\theta_e, \theta_i = 15$ mV, $\tau = 50$ ms, $\alpha = 50\ \mathrm{s}^{-1}$, $\beta = 200\ \mathrm{s}^{-1}$, $\gamma_e = 100$ Hz, $\sigma = 6$ mV, $\varphi_n = 2$ mV s, $\nu_{ei} = 1.8$ mV s, $\nu_{es} = 1.8$ mV s, $\nu_{d_1e} = 1$ mV s, $\nu_{d_2e} = 0.7$ mV s, $\nu_{d_2s} =$ 0.05 mV s, $\nu_{d_1s} = 0.1$ mV s, $\nu_{d_2d_2} = 0.3$ mV s, $\nu_{d_1d_1} = 0.2$ mV s, $\nu_{ee} = 1$ mV s, $\nu_{p_1p_2} = 0.03$ mV s, $\nu_{\varsigma e} = 0.1$ mV s, $\nu_{p_1\varsigma} = 0.1$ mV s, $\nu_{re} = 0.05$ mV s, $\nu_{p_2\varsigma} = 0.45$ mV s, $\nu_{sp_1} = 0.035$ mV s, $\nu_{\varsigma p_2} =$ 0.04 mV s, $v_{rs} = 0.5$ mV s, $\nu_{p_1d_1} = 0.1$ mV s, $\nu_{se} = 2.2$ mV s, $\nu_{p_2p_2} = 0.075$ mV s, $\nu_{p_2d_2} = 0.3$ mV s, $\nu_{rp_1} = 0.035$ mV s.

3. Main results

Figure 2a describes the transition process between different states caused by changing $-\nu_{sr}$. We find that four distinct states appear successively in the EPN with increasing $-\nu_{sr}$: saturated state D; epilepsy state C; simple periodic oscillation state B; and low firing state A. Figure 2b–e show four time-series diagrams, which are simulated by taking $-\nu_{sr} = 0.5$, $-\nu_{sr} = 1.2$, $-\nu_{sr} = 1.5$ and $-\nu_{sr} =$ 2.2, respectively, in Fig. 2a. Saturation state D refers to a firing rate of 250 Hz (i.e., $Q_e^{\max}$), which may be an idealized state that only appears in theoretical model studies. Seizure state C is a kind of periodic oscillation phenomenon; in each cycle, four extreme points can be found in the oscillation. State B is a periodic activity, the morphology of which is similar to a sinusoidal wave, and is a transition state between A and C that may be induced by a Hopf bifurcation. State A is a low frequency firing pattern in the brain.

Now, we apply an external stimulation voltage V on the target STN to consider the mechanism for controlling AE by changing the stimulus intensity. Figure 2f represents the state bifurcation diagram for this situation. From Fig. 2f, we can see that when $-\nu_{sr}$ is small, AE might be suppressed by properly

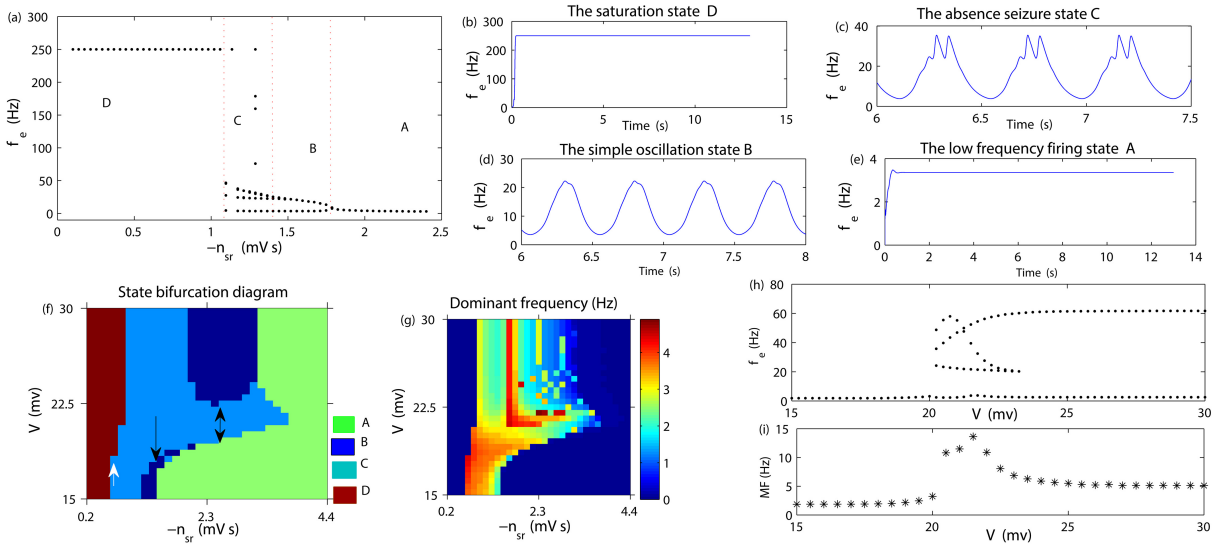

Fig. 2. (a): Brain state transition diagram caused by changing $-\nu_{sr}$. (b)–(e): Four time series diagrams. All simulations in (a)–(e), we set $\tau = 0.12$ s; $\nu_{p_1\zeta} = 0.2$; $V = 0$; $\nu_{ee} = 1.6$; $\nu_{re} = 0.07$; $\nu_{rs} = 0.7$; $\nu_{d_1d_1} = 0.3$; $\nu_{d_2d_2} = 0.4$; ν_{es} =1.4; $\nu_{se} = 2.6$; $\nu_{sp_1} = 0.034$; and $\nu_{rp_1} = 0.03$. (f) and (g): The state bifurcation and DF simulations in $(-\nu_{sr}, V)$. (h): One typical bifurcation process of ϕ_e. (i): A simulation of MF, corresponding to (h).

enhancing (the upward arrow) or lowering (the downward arrow) the voltage in the seizure area. An interesting two-way regulation phenomenon appears when $-\nu_{sr}$ increases to a sufficiently large value (indicated by the double arrow). This phenomenon may be induced by a competitive mechanism between ν_{sp_1} and ν_{rp_1}. In combination with Fig. 2f, it is not difficult to find that the range of oscillatory dominant frequency (DF) is mainly approximately 2–4 Hz in Fig. 2g. When we set $-\nu_{sr} = 3$ mV s, a typical transfer process is obtained, as seen in Fig. 2h, which illustrate an obvious bifurcation process among states A, B and C. Figure 2i is the corresponding average discharge rate (MF) of the EPN as a function of V, which compares well to the trend seen in Fig. 2h.

4. Conclusion

The whole society should pay great attention to the care and treatment of epileptic patients. Externally invasive treatment is an important scheme in controlling intractable epilepsy, such as DBS. However, the relative mechanism is unknown, and theoretical results on the control effect of uniform direct current stimulation are still lacking. In this paper, by using a cortical thalamic-BG network, we investigated the control mechanism of AE by varying the intensity of the stimulus voltage. From the numerical simulation result, it can be seen that the seizure was relieved via reasonably adjusting the intensity of the stimulus, which may be realized through the mutual competitions between the projections in "*SNr* $\rightarrow$ *TRN*" and "*SNr* $\rightarrow$ *SRN*", in some cases, there appear interesting two-way adjustments. From the two angles of the theoretical model and numerical calculation, we can understand these control mechanisms very well. Because the stimulation voltage may be easily adjusted in clinical practice, the results may inspire clinical and experimental studies in the future.

The mean field equation is the simplified mathematical model to reflect the biological phenomena, the advantages of which are tractable. However, it cannot describe a more complex brain physiological environment, such as ion channel concentration, receptor activation level, and network connection structure.

Moreover, the absence seizure activities are observed to be synchronous in the brain. Therefore, in the partial differential equations used in this paper, we have omitted the spatial derivative for simplification. In this paper, we chose the STN as the stimulation target area. Future studies may be interested in the choice of the optimal target and the optimal stimulation scheme. All these should resort to the spike network. As the results can be applied to specific patients, future research can also resort to data-driven approaches, such as high-throughput omics data and network biomarkers, which can also be applied to similar fields.

Acknowledgments

This research was supported by the National Science Foundation of China (no. 11602092), the Natural Science Foundation of Hubei Province (no. 2018CFB628), and the China Postdoctoral Science Foundation (no. 2018M632184).

Conflict of interest

None to report.

References

[1] Loiseau P, Duché B, Pédespan JM. Absence epilepsies. Epilepsia. 1995; 36(12): 1182-1186.
[2] Crunelli V, Leresche N. Childhood absence epilepsy: Genes, channels, neurons and networks. Nat Rev Neurosci. 2002; 3(5): 371.
[3] Rodrigues S, Barton D, Szalai R, et al. Transitions to spike-wave oscillations and epileptic dynamics in a human cortico-thalamic mean-field model. J Comput Neurosci. 2009; 27(3): 507-526.
[4] Case M, Soltesz I. Computational modeling of epilepsy. Epilepsia. 2011; 52(s8): 12-15.
[5] Dadok VM, Szeri AJ, Kirsch H, et al. Interpretation of seizure evolution pathways via a mean-field cortical model. BMC Neurosci. 2012; 13(1): 95.
[6] Marten F, Rodrigues S, Benjamin O, et al. Onset of polyspike complexes in a mean-field model of human electroencephalography and its application to absence epilepsy. Philos Trans R Soc, A. 2009; 367(1891): 1145-1161.
[7] Marten F, Rodrigues S, Suffczynski P, et al. Derivation and analysis of an ordinary differential equation mean-field model for studying clinically recorded epilepsy dynamics. Phys Rev E. 2009; 79(2): 021911.
[8] Chen MM, Guo DQ, Wang TB, et al. Bidirectional control of absence seizures by the basal ganglia: A computational evidence. PLoS Comput Biol. 2014; 10(3): e1003495.
[9] Hu B, Guo D, Wang Q. Control of absence seizures induced by the pathways connected to SRN in corticothalamic system. Cogn Neurodynamics. 2015; 9(3): 279-289.
[10] Child ND, Stead M, Wirrell EC, et al. Chronic subthreshold subdural cortical stimulation for the treatment of focal epilepsy originating from eloquent cortex. Epilepsia. 2014; 55(3): e18-e21.
[11] Vesper J, Steinhoff B, Rona S, et al. Chronic high-frequency deep brain stimulationof the STN/SNr for progressive myoclonic epilepsy. Epilepsia. 2007; 48(10): 1984-1989.
[12] Jou SB, Kao IF, Yi PL, et al. Electrical stimulation of left anterior thalamic nucleus with high-frequency and low-intensity currents reduces the rate of pilocarpine-induced epilepsy in rats. Seizure. 2013; 22(3): 221-229.
[13] Feng L, Liu TT, Ye DW, et al. Stimulation of the dorsal portion of subthalamic nucleus may be a viable therapeutic approach in pharmacoresistant epilepsy: A virally mediated transsynaptic tracing study in transgenic mouse model. Epilepsy Behav. 2014; 31: 114-116.
[14] Pasnicu A, Denoyer Y, Haegelen C, et al. Modulation of paroxysmal activity in focal cortical dysplasia by centromedian thalamic nucleus stimulation. Epilepsy Res. 2013; (3): 264-268.
[15] Chen M, Guo D, Li M, et al. Critical roles of the direct GABAergic pallido-cortical pathway in controlling absence seizures. PLoS Comput Biol. 2015; 11(10): e1004539.

[16] Sorokin JM, Davidson TJ, Frechette E, et al. Bidirectional control of generalized epilepsy networks via rapid real-time switching of firing mode. Neuron. 2017; 93(1): 194-210.
[17] Hu B, Chen S, Chi H, et al. Controlling absence seizures by tuning activation level of the thalamus and striatum. Chaos Soliton Fract. 2017; 95: 65-76.
[18] Ghai RS, Bikson M, Durand DM. Effects of applied electric fields on low-calcium epileptiform activity in the CA1 region of rat hippocampal slices. J Neurophysiol. 2000; 84(1): 274-280.
[19] Radman T, Ramos RL, Brumberg JC, et al. Role of cortical cell type and morphology in subthreshold and suprathreshold uniform electric field stimulation *in vitro*. Brain Stimul. 2009; 2(4): 215-228.
[20] Liebetanz D, Klinker F, Hering D, et al. Anticonvulsant effects of transcranial direct-current stimulation (tDCS) in the rat cortical ramp model of focal epilepsy. Epilepsia. 2006; 47(7): 1216-1224.
[21] Bui AD, Alexander A, Soltesz I. Seizing control: From current treatments to optogenetic interventions in epilepsy. The Neuroscientist. 2017; 23(1): 68-81.
[22] Paz JT, Davidson TJ, Frechette ES, et al. Closed-loop optogenetic control of thalamus as a tool for interrupting seizures after cortical injury. Nat Neurosci. 2013; 16(1): 64-70.
[23] van Albada SJ, Gray RT, Drysdale PM, et al. Mean-field modeling of the basal ganglia-thalamocortical system. II: Dynamics of parkinsonian oscillations. J Theor Biol. 2009; 257(4): 664-688.